Why the atomic spins point the way they do

by

Raquel Lizárraga Jurado

Licentiate Thesis in Physics
Uppsala University, 2003

Abstract

Non-collinear density functional theory and its application to particular physical problems are discussed in this thesis. The magnetic structure of the compound $TlCo_2Se_2$ is investigated and an electronic structure analysis is presented. Features of the Fermi surface and details in the band structure are argued to be involved in the stabilization of a non-collinear incommensurate magnetic structure as the ground state of $TlCo_2Se_2$. Two criteria are identified that determine whether a magnetic metal will be in a collinear, i.e. ferromagnetic state or in a non-collinear state like in a spin spiral arrangement. Our analysis shows that a non-collinear state can be stabilized in any element or compound provided the band filling and exchange splitting are tuned correctly.

List of Publications

This thesis is based on the collection of papers given below. Each article will be referred to by its Roman numeral.

I) **A theoretical and experimental study of the magnetic structure of $TlCo_2Se_2$**
R. Lizárraga, S. Ronneteg, R. Berger, A. Bergman, O. Eriksson and L. Nordström

II) **Why the atomic spins point the way they do**
R. Lizárraga, L. Nordström, L. Bergqvist, A. Bergman, E. Sjöstedt, P. Mohn and O. Eriksson

Contents

Chapter 1

Introduction

The discovery of magnets lies far back in the elder days. The legend of a shepherd named Magnes who while tending his sheep on the slopes of the mount Ida in Crete, found that his iron tipped crook and the nails of his boots were attracted to the ground, is probably the earliest account we have concerning magnets. The magical powers of magnetite, as the stone Magnes had stepped on was called later, are mentioned in the writings of the Roman encyclopedist Pliny the Elder (23-79 a.c.). For many years after its discovery, magnetite was surrounded by superstition. The skills of healing the sick, frightening away evil spirits and attracting and dissolving ships made of iron, were some of the prodigies associated to magnetite. As in many other subjects of the human knowledge, the supernatural influences and divine intervention were left behind when the work of scientists like Oersted (1777-1851) and later on James Clerk Maxwell (1831-1879) contributed to cast light on the phenomenon of magnetism and electromagnetism. Since the Chinese compass (III century b.c.), which is the first known application of magnetism, the technological interest in magnetic materials has grown immensely. The storage media like the hard disk in our computers, floppy disks, tapes and permanent magnets in electric motors are some of the practical uses of magnetism in our every day lives. It is, therefore, in the field of condensed matter where magnetism has caused the major interest in the last decades.

The manifestation of magnetism in solid state physics is a matter of importance in this thesis, particularly the arrangement of the magnetic moments that gives rise to what is not a very common magnetic structure; spin spirals. Magnetic materials are often found to be ferromagnets or antiferromagnets, i.e. magnetic moments pointing parallel or anti-parallel along certain global quantization axis. However, in rare occasions, they are orientated in such a manner that there is no global quantization axis. The latter is called non-collinear magnetism and spin spirals are examples of it. Why the spins choose to order either in a collinear way like in ferromagnets and antiferromagnets or in a non-collinear way is a question that has not found a complete answer yet. Before embarking on the discussion of this issue -in fact, the second part of chapter five is devoted to this matter- we will remark in

this introduction some basis facts of magnetism, going all the way through from a single electron until it is placed with other electrons in an atom or in a solid.

1.1 Magnetism in Condensed Matter

The fundamental object in magnetism is the magnetic moment, which in classical electromagnetism, is defined as

$$\mathrm{d}\boldsymbol{\mu} = I\mathrm{d}\mathbf{a} \tag{1.1}$$

where I is a current around an elementary oriented loop of area $|\mathrm{d}\mathbf{a}|$. The direction of the vector $\mathrm{d}\mathbf{a}$ is normal to the loop and determined by the direction of the current around the elementary loop (the screw rule). Consequently, the magnetic moment can be either parallel or anti-parallel to the angular momentum vector associated with the charge that is going around the loop.

When applying a magnetic field to a system of interacting electrons, an induced magnetization appears. We could try to calculate the net magnetic moment of this system in a classical manner and then complete the description with the appropriate quantum mechanical corrections. However, Bohr and Van Leeuwen showed that magnetism can not be understood in the framework of a classical theory based in the magnetism of moving charges. Consequently, a quantum mechanical description is necessary in order to give full account of magnetism. Hence, the intrinsic angular momentum or spin of the electrons must be considered, which is characterized by the spin quantum number $s = 1/2$. The spin angular momentum is as well associated with an intrinsic magnetic moment $\boldsymbol{\mu}_s = -g\mu_{\mathrm{B}}\mathbf{s}$. In this expression $g \approx 2$ is a constant known as the g-factor and μ_{B} is the Bohr magneton. The energy of the magnetic moment in a magnetic field, $\mathbf{B}$, is $-\boldsymbol{\mu}\cdot\mathbf{B}$, so that the energy is minimized when the magnetic moment lies along the magnetic field direction. If we consider a magnetic field in the z direction, the energy levels of an electron split in a magnetic field by an amount $g\mu_{\mathrm{B}}B$, the so called Zeeman splitting.

The Hamiltonian that describes an atom with Z electrons moving in a potential V and a magnetic field includes the Zeeman term and it is written as [1, 2]

$$\begin{aligned}
\mathcal{H} &= \sum_{i=1}^{Z}\left(\frac{1}{2m}\left(\mathbf{p}_i + \frac{e}{c}\mathbf{A}_i\right)^2 + V(\mathbf{r}_i) + g\mu_{\mathrm{B}}\mathbf{B}\cdot\mathbf{s}_i\right) + \frac{1}{2}\sum_{i\neq j}\frac{e^2}{|\mathbf{r}_i - \mathbf{r}_j|} \\
&= \sum_{i=1}^{Z}\left(\frac{\mathbf{p}_i^2}{2m} + V(\mathbf{r}_i) + \mu_{\mathrm{B}}\mathbf{B}\cdot(\boldsymbol{\sigma}_i + \boldsymbol{\ell}_i) + \frac{e^2}{8mc^2}(\mathbf{B}\times\mathbf{r}_i)^2\right) \\
&+ \frac{1}{2}\sum_{i\neq j}\frac{e^2}{|\mathbf{r}_i - \mathbf{r}_j|}.
\end{aligned} \tag{1.2}$$

When deriving the Hamiltonian in Eqn (1.2), first, the momentum $\mathbf{p}_i$ of each electron is replaced by $(\mathbf{p}_i + e\mathbf{A}_i/c)$, as an effect of the magnetic field,[1] where the

[1] In a purely classical theory this would be the only effect of the field.

gauge is chosen in such way that the potential $\mathbf{A}$ is equal to $(\mathbf{B} \times \mathbf{r}_i)/2$. Secondly, the definitions of the spin and the angular momentum

$$\mathbf{s}_i = \frac{\boldsymbol{\sigma}_i}{2} \qquad \text{and} \qquad \hbar\boldsymbol{\ell} = \mathbf{r}_i \times \mathbf{p}_i, \tag{1.3}$$

were used, where $\boldsymbol{\sigma}$ is the Pauli spin matrix vector. Finally, relativistic corrections were not included. From quantum mechanics we know that everything we could know about the system, described by the Hamiltonian in Eqn(1.2), can be found by solving the time-independent Schrödinger equation

$$\mathcal{H}\Psi = \varepsilon\Psi, \tag{1.4}$$

where Ψ is the total wave function of the whole system. The problem of three bodies is already unsolvable and therefore this approach is intractable for atoms with the exception of hydrogen, unless we incorporate some approximations.

Hartree introduced a high-yielding concept which appeals to the variational principle of the quantum mechanics. The principle establishes that the total energy,

$$E = \langle\Phi|\mathcal{H}|\Phi\rangle = \int \Phi^*\mathcal{H}\,\Phi\,\mathrm{d}\mathbf{r}, \tag{1.5}$$

is stationary with respect to variation of Φ, and that E is always an upper bound to the ground state energy. In Eqn (1.5) Φ is an approximate but normalized wave function that has the appropriate form of the electron system under investigation. Clearly if Φ were the exact ground state wave function then E would be the ground state energy. By writing the wave function Φ as a determinant of single-particle wave functions ϕ_i, the variation of E with respect to the single-particle wave functions leads to the Euler equations, the so-called Hartree-Fock equations[2],

$$\begin{aligned}\left(-\frac{\hbar^2}{2m}\nabla^2 + V(\mathbf{r})\right)\phi_n(\mathbf{r}) + \sum_{j=1}^{N}\int \phi_j^*(\mathbf{r}')\phi_j(\mathbf{r}')\frac{e^2}{|\mathbf{r}-\mathbf{r}'|}\mathrm{d}\mathbf{r}'\,\phi_n(\mathbf{r}) \\ -\sum_{j=1}^{N}\int \phi_j^*(\mathbf{r}')\phi_n(\mathbf{r}')\frac{e^2}{|\mathbf{r}-\mathbf{r}'|}\,\mathrm{d}\mathbf{r}'\,\phi_j(\mathbf{r})\,\delta_{S_jS_n} = \varepsilon_n\,\phi_n(\mathbf{r}).\end{aligned} \tag{1.6}$$

The last term on the left hand side of Eqn (1.6) is called the exchange potential and even though it is Coulombic, its origin is quantum mechanical. It is possible to see in Eqn (1.6) that the terms $j = n$ in both sums cancel each other. Moreover if we neglect the last term in Eqn (1.6) which singles out those electrons with spins of state j parallel to the state n, we obtain the Hartree equations. They represent an electron moving in an effective or averaged potential due to the all other electrons. The Hartree-Fock approximation has turned out to give very accurate agreement with experiments for atoms.

[2]The derivation of the Hartree-Fock equations can be found in any solid state book like for instance in Refs. [2, 3, 4].

However, in solids, where the electronic density is very high, this approximation becomes less helpful. First principles calculations based on density functional theory (DFT) present an accurate and reliable way to obtain ground state properties of solids. The essential point is to replace the complication of calculating the total wave function of the many-body problem by the problem of finding the ground state density [3]. DFT adds effects of exchange and correlation to the Hartree-type Coulomb terms to describe electron-electron interaction. This theory has also been extended to the spin-polarized case which permits us to investigate magnetic systems. Exchange interactions favour magnetic solutions since they keep electrons of the same spin apart due to the Pauli exclusion principle decreasing the Coulomb energy while the kinetic energy will favour a non-magnetic solution. Therefore the driving mechanism that produces magnetism is the lowering of the Coulomb energy due to exchange.

The rest of this thesis is organized as follows. The second chapter describes the main aspects of DFT with a special emphasis on non-collinear magnetism. The third chapter contains a brief account of the computational method, augmented planewave plus local orbitals (APW+lo), which has produced almost all the results presented in this thesis. The chapter four is devoted to some of the more important aspects of non-collinear magnetism which will be reviewed in connection to the manuscripts attached at the end of the thesis. Finally, the results of this investigation will be shown in chapter five.

[3] A more detailed description of density functional theory will be given in the next chapter.

Chapter 2

Density Functional Theory

2.1 The many-body problem

Since our concern here is the understanding of real materials we must describe atoms that are condensed to form a solid. As we indicated in the introduction of this thesis the way of doing this is solving the Schrödinger equation

$$\mathcal{H}\Psi = \mathcal{E}\Psi, \tag{2.1}$$

of a system containing nuclei and electrons. The total energy of such a system is $\mathcal{E}$, Ψ is the total wave function which contains information of the whole system and $\mathcal{H}$ is the Hamiltonian that can be written out as

$$\begin{aligned}\mathcal{H} \;= &\sum_{\mu}\Big[-\frac{\hbar^2}{2M_\mu}\nabla_\mu^2+\sum_{\nu>\mu}V_I(\mathbf{X}_\mu-\mathbf{X}_\nu)\Big]+\sum_i\Big[-\frac{\hbar^2}{2m}\nabla_i^2\\ &+\sum_{j>i}\frac{e^2}{|\mathbf{r}_i-\mathbf{r}_j|}+\sum_\mu U_{\text{e-I}}(\mathbf{r}_i-\mathbf{X}_\mu)\Big].\end{aligned} \tag{2.2}$$

where $\mathbf{X}_\mu$ and $\mathbf{r}_i$ are the coordinates of the nuclei and electrons, whereas M_μ and m_i stand for the masses of the nuclei and the electrons, respectively. The first and the third term in the Hamiltonian given in Eqn (2.2) are the kinetic energy of the nuclei and the electrons, respectively. The quantity $V_I(\mathbf{X}_\mu - \mathbf{X}_\nu)$ is the interaction potential of the nuclei with each other, while $U_{\text{e-I}}(\mathbf{r}_i - \mathbf{X}_\mu)$ represents the interaction between an electron at $\mathbf{r}_i$ and a nucleus at $\mathbf{X}_\mu$. Although Eqn (2.1) looks simple it is not possible to solve for solids, in particular metals, whose density of conduction electrons is very high ($\sim 10^{23}/\text{cm}^3$). The Born-Oppenheimer approximation provides us with a way of simplifying our Hamiltonian and states that because the electrons are much lighter than the nuclei they move much more rapidly and can follow the slower motions of the nuclei quite accurately. This fact allows us to discuss the motion of the electrons separately from the motion of the

nuclei. The Born-Oppenheimer approximation leaves us with an electronic Hamiltonian which is less complicated, but does not unburden us of the electron-electron term which makes the Schrödinger equation unsolvable. The complexity of the many-body problem then forces us to get another route towards the understanding of solids.

2.2 Density Functional Theory

A significant reduction of the complicated many-body problem stated in the previous section was supplied by the density functional theory (DFT) due to Hohenberg and Kohn [5] and Kohn and Sham [6]. The essential point of DFT is the realization that the ground state density is sufficient to calculate all physical quantities of interest. Therefore, instead of calculating the many-body wave function Ψ, the knowledge of the ground-state density becomes crucial. DFT is based in the following two theorems established by Hohenberg and Kohn,

Theorem 1 *The total ground-state energy, E, of a many-electron system is a functional of the density*

$$n(\mathbf{r}) = \langle \Psi | \hat{n}(\mathbf{r}) | \Psi \rangle \tag{2.3}$$

where $|\Psi\rangle$ is a many-body state and $\hat{n}$ is the electron-density operator.

Theorem 2 *The functional $E[n]$ of a many-electron system has a minimum equal to the the ground state energy at the ground state density.*

The proof of these theorems as well as v-representability issues will not be given here but the interested reader can find detailed information in ref.[7, 8, 9]. Unfortunately these theorems provide no information about the form of the functional $\mathrm{E}[n]$ and therefore the utility of DFT relies upon our ability to find accurate approximations. Kohn and Sham (1965) used the variational principle implied by the second theorem to derive the single-particle Schrödinger equations. In order to see this we proceed by writing the total energy functional, $\mathrm{E}[n]$ as [1]

$$\mathrm{E}\left[n\right] = \mathrm{T}\left[n\right] + \int n(\mathbf{r}) v_{\text{ext}}(\mathbf{r})\, \mathrm{d}\mathbf{r} + \iint \frac{n(\mathbf{r}) n(\mathbf{r}')}{|\mathbf{r} - \mathbf{r}'|}\, \mathrm{d}\mathbf{r}\, \mathrm{d}\mathbf{r}' + \mathrm{E}_{\text{xc}}\left[n\right] , \tag{2.4}$$

which contains the kinetic, the external potential which in the Born-Oppenheimer approximation is the potential due to the ions, the Hartree component of the electron-electron energy and the exchange correlation energy. The last term is actually a receptacle of our lack of knowledge of the contribution of the many-body interactions to the total energy. Although an explicit form of T and E_{xc} in Eqn (2.4) is not known in general, we use the variational principle on the total energy functional to write

$$\frac{\delta \mathrm{E}\left[n\right]}{\delta n(\mathbf{r})} + \mu \frac{\delta(\mathrm{N} - \int n(\mathbf{r})\, \mathrm{d}\mathbf{r})}{\delta n(\mathbf{r})} = 0, \tag{2.5}$$

[1] Hereafter atomic Rydberg units (a.u.) will be used.

where μ is a Lagrange multiplier which takes care of the particle conservation. Since we know the expression of the kinetic energy of non-interacting particles $\mathrm{T}_0[n]$, it is convenient to split up the kinetic energy term in Eqn (2.4) into two terms $\mathrm{T} = \mathrm{T}_0 + \mathrm{T}_{\mathrm{xc}}$, where T_{xc} stands for the exchange-correlation part of the kinetic energy. Finally by using the density [2]

$$n(\mathbf{r}) = \sum_{i=1}^{N} |\psi_i(\mathbf{r})|^2 , \tag{2.6}$$

where the sum extends over the lowest N-occupied states, we are able to determine the functional derivatives in Eqn (2.5). This procedure yields a set of effective single-particle equations called the Konh-Sham equations [3]

$$\left[-\nabla^2 + v_{\mathrm{eff}}(\mathbf{r}) - \varepsilon_i\right] \psi_i(\mathbf{r}) = 0, \tag{2.7}$$

which are Schrödinger equations where the external potential has been replaced by an effective potential defined by

$$v_{\mathrm{eff}}(\mathbf{r}) = v_{\mathrm{ext}}(\mathbf{r}) + 2\int \frac{n(\mathbf{r}')}{|\mathbf{r}-\mathbf{r}'|}\,\mathrm{d}\mathbf{r}' + v_{\mathrm{xc}}(\mathbf{r}), \tag{2.8}$$

with the exchange-correlation potential

$$v_{\mathrm{xc}}(\mathbf{r}) = \frac{\delta(\mathrm{E}_{\mathrm{xc}}[n])}{\delta n(\mathbf{r})}. \tag{2.9}$$

In Eqn (2.9), E_{xc} contains now the exchange-correlation part of the kinetic energy T_{xc}. The eigenvalues ε_i obtained above are not in general simply related to measured quantities hence their physical meaning is still controversial [4].

2.3 Local Density Approximation

Density functional theory as outlined above supplies a scheme to map the many-body problem into a Schrödinger-like effective single-particle equation provided we introduce an approximation to the exchange-correlation functional. The so-called local density approximation (LDA) achieves this task by making use of the homogeneous, interacting electron gas to model the exchange-correlation energy

$$\mathrm{E}_{\mathrm{xc}} = \int n(\mathbf{r})\epsilon_{\mathrm{xc}}(n(\mathbf{r}))\,\mathrm{d}\mathbf{r}, \tag{2.10}$$

[2] Here we will simply assume that we can determine single-particle wave functions $\{\psi_i(\mathbf{r})\}$ which permit us to express the density as in Eqn (2.6) leaving further disquisitions to the specialized literature.

[3] A full derivation of the Kohn-Sham equations will not be given here but it can be easily found in ref. [7, 8, 9]

assuming that ϵ_{xc} is approximated by a local function of the density, usually that which reproduces the known energy of the uniform electron gas. There are attempts to refine LDA, for instance the generalized gradient approximation (GGA) and the weighted density approximation (WDA). An expression similar to which is shown in Eqn (2.10) is used in GGA but in this case ϵ_{xc} is a function of the gradient of the density $|\nabla n(\mathbf{r})|$ as well as the density $n(\mathbf{r})$ [10, 11, 12]. The WDA [13, 14, 15] is a more sophisticated approach, that incorporates true non-local information through Coulomb integrals of the density with model exchange correlation holes. Although WDA improves greatly the energy of atoms it is more computationally demanding than LDA or GGA and therefore there are very few reports in the literature of WDA applied to solids. In contrast, GGA has been widely used in first principles calculations but despite its success in predicting the bcc ground state of Fe [4] , it has not been found to improve significantly LDA calculations in metallic magnets, at least not as concerns the ground state magnetic properties.

2.4 Spin density functional theory

So far we have discussed DFT for non-spin-polarized systems and since the work presented in this thesis concerns magnetic materials we now turn into the description of the spin density functional theory (SDFT). We will omit details for they are essentially similar to what was discussed in the former sections, emphasizing those features that are typical for the SDFT, in particular its applications to the study of non-collinear magnets. [5]

In 1972 von Barth and Hedin [16] extended the DFT to the spin polarize case. They used a 2×2 matrix formalism to represent the density and the external potential instead of single variables.

$$n(\mathbf{r}) \qquad \Longrightarrow \qquad \rho(\mathbf{r}) = \begin{pmatrix} \rho_{11} & \rho_{12} \\ \rho_{21} & \rho_{22} \end{pmatrix} \tag{2.11}$$

$$v_{\text{ext}}(\mathbf{r}) \qquad \Longrightarrow \qquad \tilde{v}_{\text{ext}}(\mathbf{r}) = \begin{pmatrix} v_{11}^{\text{ext}} & v_{12}^{\text{ext}} \\ v_{21}^{\text{ext}} & v_{22}^{\text{ext}} \end{pmatrix} \tag{2.12}$$

We begin our discussion by noticing that the wave functions will adopt the form of spinors,

$$\psi_i(\mathbf{r}) = \begin{pmatrix} \phi_{i\alpha}(\mathbf{r}) \\ \phi_{i\beta}(\mathbf{r}) \end{pmatrix}, \tag{2.13}$$

where $\phi_{i\alpha}$ and $\phi_{i\beta}$ are the two spin projections. In the non-spin polarized case we defined the density (see Eqn (2.6)) as the sum of $|\psi_i|^2$ extended over the lowest N-occupied states. We now write the matrix elements of the density matrix ρ in

[4] LDA fails in reproducing this result.

[5] Although SDFT was formulated completely general, its earlier implementations were mostly done for the special case of diagonal matrices, i.e. collinear magnetism.

Eqn (2.11) as

$$\rho_{\alpha\beta}(\mathbf{r}) = \sum_{\substack{i=1 \\ \varepsilon_{i\alpha},\varepsilon_{i\beta}\leq E_{\mathrm{F}}}}^{N} \phi_{i\alpha}(\mathbf{r})\,\phi^{*}_{i\beta}(\mathbf{r})\,. \tag{2.14}$$

The next step is to write down the total energy that now is a functional of ρ and subsequently derive the single-particle equations,

$$\mathrm{E}\left[\rho\right] = \mathrm{T}\left[\rho\right] + \mathrm{V}_{\mathrm{ext}}[\rho] + \iint \frac{n(\mathbf{r})n(\mathbf{r}')}{|\mathbf{r}-\mathbf{r}'|}\,\mathrm{d}\mathbf{r}\,\mathrm{d}\mathbf{r}' + \mathrm{E}_{\mathrm{xc}}\left[\rho\right]\,. \tag{2.15}$$

The external potential $V_{\mathrm{ext}}\left[\rho\right]$ in Eqn (2.15) is the potential due the ions specified by

$$\sum_{\alpha\beta}\int n_{\alpha\beta}(\mathbf{r})\,v^{\mathrm{ext}}_{\alpha\beta}(\mathbf{r})\,\mathrm{d}\mathbf{r}\,. \tag{2.16}$$

By appealing to the variational principle again

$$\frac{\delta \mathrm{E}\left[\rho\right]}{\delta\rho_{\alpha\beta}(\mathbf{r})} = 0, \tag{2.17}$$

and proceeding in the same way as in the non-polarized case we derive the single-particle equations which constitute the Kohn-Sham equations for a spin system,

$$\sum_{\beta}\left(-\delta_{\alpha\beta}\nabla^2 + v^{\mathrm{eff}}_{\alpha\beta}\left(\mathbf{r}\right) - \varepsilon_i\delta_{\alpha\beta}\right)\phi_{i\beta}(\mathbf{r}) = 0, \tag{2.18}$$

where no assumption of collinearity, i.e. all spin parallel or anti parallel to a global quantization axis, has been made. The effective potential matrix elements in Eqn (2.18) can be written down as

$$v^{\mathrm{eff}}_{\alpha\beta}(\mathbf{r}) = v^{\mathrm{ext}}_{\alpha\beta}(\mathbf{r}) + 2\delta_{\alpha\beta}\int \frac{n(\mathbf{r}')}{|\mathbf{r}-\mathbf{r}'|}\,\mathrm{d}\mathbf{r}' + v^{\mathrm{xc}}_{\alpha\beta}(\mathbf{r}). \tag{2.19}$$

with the exchange-correlation potential matrix elements

$$v^{\mathrm{xc}}_{\alpha\beta}(\mathbf{r}) = \frac{\delta(\mathrm{E}_{\mathrm{xc}}[\rho])}{\delta\rho_{\alpha\beta}(\mathbf{r})}\,. \tag{2.20}$$

2.5 Non-uniformly magnetized systems

The application of SDFT as well as its non-spin-polarized partner's requires the introduction of an approximation that allows us to deal with the exchange-correlation functional. LDA can be readily generalized to the spin-polarized case (LSDA) [16] by defining spin-up and spin-down densities, however the aim of this section is to include in our discussion also those cases where there is no global spin quantization axis, i.e. non-collinear magnetization. Hence the discussion presented here will be established in a general way.

In the previous section we learnt that SDFT uses a 2×2 matrix formalism. The density matrix (see Eqn (2.14) was defined as

$$\rho(\mathbf{r}) = \sum_{i=1}^{N} \begin{pmatrix} |\phi_{i\alpha}(\mathbf{r})|^2 & \phi_{i\alpha}(\mathbf{r})\phi^*_{i\beta}(\mathbf{r}) \\ \phi^*_{i\alpha}(\mathbf{r})\phi_{i\beta}(\mathbf{r}) & |\phi_{i\beta}(\mathbf{r})|^2 \end{pmatrix}, \tag{2.21}$$

which generally can be expanded in terms of the density $n(\mathbf{r})$ and the magnetization density $\mathbf{m}(\mathbf{r})$, that is naturally a vector density,

$$\rho(\mathbf{r}) = \frac{1}{2}\left[n(\mathbf{r})\mathbb{1} + \mathbf{m}(\mathbf{r}) \cdot \boldsymbol{\sigma}\right], \tag{2.22}$$

where $\mathbb{1}$ is the 2×2 unit matrix and $\boldsymbol{\sigma} = (\sigma_x, \sigma_y, \sigma_z)$ are the Pauli matrices. The electronic and the magnetization density are then expressed as

$$n(\mathbf{r}) = Tr(\rho(\mathbf{r})) = \sum_{i=1}^{N} |\psi_i|^2 \qquad \text{and} \qquad \mathbf{m}(\mathbf{r}) = \sum_{i=1}^{N} \psi_i{}^{\dagger} \boldsymbol{\sigma} \psi_i, \tag{2.23}$$

where the sum in Eqn (2.23) extends over the lowest occupied states. In the simplest case where the spins are arranged in a collinear way, the density matrix is diagonal and therefore the magnetization becomes,

$$m_z(\mathbf{r}) \;=\; \sum_{i=1}^{N} \left[|\phi_{i\alpha}|^2 - |\phi_{i\beta}|^2 \right] = \sum_{i=1}^{N} \left[n_{\uparrow}(\mathbf{r}) - n_{\downarrow}(\mathbf{r}) \right]. \tag{2.24}$$

In (Eqn 2.24) it was assumed the global magnetization axis to be in the z-direction and the eigenvalues of the diagonal density matrix to be $n_{\uparrow}$ (spin-up density) and $n_{\downarrow}$ (spin-down density). The exchange correlation energy, in Eqn (2.10) then depends on both spin densities, $\epsilon_{\text{xc}}(n_{\uparrow}, n_{\downarrow})$ and corresponds to the exchange-correlation energy density for a spin-polarized homogeneous electron gas. However, in a more general case, where non-diagonal matrices are considered the exchange-correlation functional may be given by

$$\mathrm{E}_{\text{xc}}\left[n(\mathbf{r}), \mathbf{m}(\mathbf{r})\right] = \int n(\mathbf{r}) \epsilon_{\text{xc}}(n(\mathbf{r}), m(\mathbf{r}))\, \mathrm{d}\mathbf{r}, \tag{2.25}$$

which permits us to determine the exchange-correlation potential (see Eqn (2.20)) as

$$v^{\text{xc}}_{\alpha\beta}(\mathbf{r}) = \frac{\delta(\mathrm{E}_{\text{xc}}[\rho])}{\delta \rho_{\alpha\beta}(\mathbf{r})} = \frac{\delta(\mathrm{E}_{\text{xc}}[\rho])}{\delta n(\mathbf{r})} \frac{\delta n(\mathbf{r})}{\delta \rho_{\alpha\beta}(\mathbf{r})} + \frac{\delta(\mathrm{E}_{\text{xc}}[\rho])}{\delta \mathbf{m}(\mathbf{r})} \frac{\delta \mathbf{m}(\mathbf{r})}{\delta \rho_{\alpha\beta}(\mathbf{r})}. \tag{2.26}$$

The first term constitutes a non-magnetic contribution to the exchange-correlation potential whereas the second term is a magnetic potential which adopts the form of a magnetic field,

$$\mathbf{b}(\mathbf{r}) = \frac{\delta(\mathrm{E_{xc}}[\rho])}{\delta \mathbf{m}(\mathbf{r})} = \frac{\delta(\mathrm{E_{xc}}[\rho])}{\delta m(\mathbf{r})}\,\hat{m}\,, \tag{2.27}$$

where $\delta m(\mathbf{r})/\delta \mathbf{m}(\mathbf{r}) = \hat{m}$ is the direction of the magnetization density. As it follows from Eqn (2.27), in LSDA the magnetic field is always parallel to the magnetization density everywhere. By combining Eqn (2.19), Eqn (2.26) and Eqn (2.27) we are now ready to write the effective potential matrix where the fact that $\delta n(\mathbf{r})/\delta\rho_{\alpha\beta}(\mathbf{r}) = \mathbb{1}$ and $\delta \mathbf{m}(\mathbf{r})/\delta\rho_{\alpha\beta}(\mathbf{r}) = \boldsymbol{\sigma}$ have been used,

$$\tilde{v}^{\mathrm{eff}}(\mathbf{r}) = v^{\mathrm{nm}}(\mathbf{r})\mathbb{1} + \mathbf{b}(\mathbf{r})\cdot\boldsymbol{\sigma}. \tag{2.28}$$

The non-magnetic term, v^{nm}, contains the external potential[6], the Hartree and the non-magnetic part of the exchange-correlation potential (Eqn 2.26),

$$v^{\mathrm{nm}}_{\alpha\beta}(\mathbf{r}) = v^{\mathrm{ext}}_{\alpha\beta}(\mathbf{r}) + 2\delta_{\alpha\beta}\int \frac{n(\mathbf{r}')}{|\mathbf{r}-\mathbf{r}'|}\,\mathrm{d}\mathbf{r}' + \delta_{\alpha\beta}\frac{\delta(\mathrm{E_{xc}}[\rho])}{\delta n(\mathbf{r})}, \tag{2.29}$$

Finally, the Kohn-Sham Hamiltonian matrix in the LSDA looks like

$$\mathcal{H} = (-\nabla^2 + v^{\mathrm{nm}})\mathbb{1} + \mathbf{b}\cdot\boldsymbol{\sigma}. \tag{2.30}$$

The non-magnetic part of the effective potential is diagonal and in the special case of a collinear system with a global magnetization axis chosen along the z-direction, the magnetic part of the potential becomes

$$\tilde{v}_{\mathrm{xc}} = \begin{pmatrix} b_z\sigma_z & 0 \\ 0 & -b_z\sigma_z \end{pmatrix}. \tag{2.31}$$

Therefore a collinear system can be treated as two separate systems, each within a effective potential $v^{\mathrm{eff}}_{\pm} = v^{\mathrm{nm}} \pm b_z\sigma_z$.

To conclude this chapter we point out that the Kohn-Sham equations, in its non-spin and spin-polarized versions, lead to a self-consistent cycle, i.e. a density must be found that produces an effective potential that once inserted in the Kohn-Sham equations yields single-particle wave functions that reproduce it. This will be discussed to some extent in the next chapter.

[6] In general, the external potential can be considered diagonal.

Chapter 3

Computational Methods

This chapter is devoted to the application of density functional theory (DFT) to real solids. In the previous chapter we found that DFT reduces the complexity of the many-body problem to an effective single-particle theory. In this framework, a set of Kohn-Sham (KS) equations are formulated and their solution entails a self-consistent cycle. That means that, a density is used to determine an effective potential, which in turns, is inserted into the Kohn-Sham equations, whose solution produces single-particle wave functions $\{\psi_i\}$, also called KS orbitals. The new set of $\{\psi_i\}$ is used to yield a new starting density. This process is repeated until the difference between the resulting density of a cycle and the respective initial density is substantially small. Then it is said that self-consistency is achieved. The procedure as outlined above normally leads to large oscillations and bad convergence of the self-consistent cycle. Hence the resulting density is always mixed in some way with the initial density to produce a new density to start the process again. The self-consistent cycle is illustrated in Fig. 3.1.

The self-consistent cycle has been implemented in many codes. Since all calculations in this thesis have been performed using a relatively new linearized form of the augmented planewave (APW) method, the so-called APW plus local orbitals (APW+lo) method, we shall describe here both the traditional linear augmented planewave method (LAPW) and APW+lo.

3.1 The secular equation

Although it is not necessary to define a basis to construct the Konh-Sham orbitals $\{\psi_i\}$ when solving the KS equations[1], it has been customary in DFT-based methods to expand $\{\psi_i\}$ in a certain basis set χ with coefficients c_{ij},

$$\psi_i(\mathbf{r}) = \sum_j c_{ij}\,\chi_j(\mathbf{r}). \tag{3.1}$$

[1] It is possible for instance, to solve numerically the differential equations on grids.

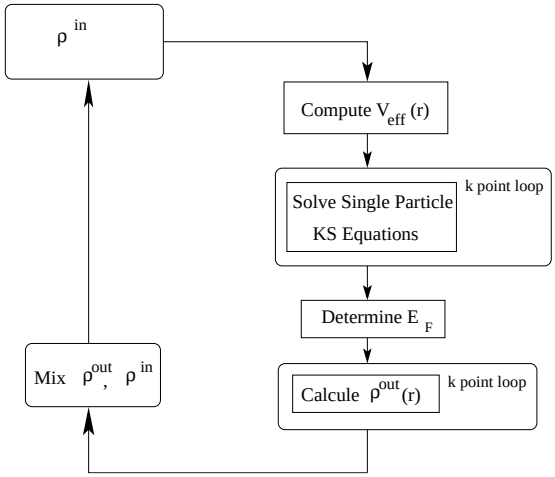

Figure 3.1: Schematic Flow-chart for self-consistent density calculations.

In Eqn (3.1) we have assumed that the Kohn-Sham orbitals can be accurately described by the basis set $\{\chi_j\}$. Unless the chosen basis set is infinitely large, this can never be achieved. Consequently the optimal c_{ij} must be obtained through a variational procedure. Thus, the KS orbitals as defined in Eqn (3.1) are inserted in the KS equations. Subsequently, by multiplying from the left by ψ^* and integrating, the resulting expression is varied,

$$\delta \sum_{jk} c_{ij}^* \, c_{ik} \left(\int \chi_j^*(\mathbf{r}) \mathcal{H} \, \chi_k(\mathbf{r}) \, \mathrm{d}\mathbf{r} - \varepsilon_i \int \chi_j*(\mathbf{r}) \chi_k(\mathbf{r}) \, \mathrm{d}\mathbf{r} \right) = 0, \tag{3.2}$$

which produces

$$\sum_{k} \left(\int \chi_j^*(\mathbf{r}) \mathcal{H} \, \chi_k(\mathbf{r}) \, \mathrm{d}\mathbf{r} - \varepsilon_i \int \chi_j^*(\mathbf{r}) \chi_k(\mathbf{r}) \, \mathrm{d}\mathbf{r} \right) c_{ij} = 0. \tag{3.3}$$

Eqn (3.3) is called the secular equation and in a matrix representation looks like

$$(H - \varepsilon_i \mathcal{O}) c_i = 0, \tag{3.4}$$

where H and $\mathcal{O}$ are the Hamiltonian and the overlap matrices respectively and c_i are vectors containing as many coefficients as the number of basis that have been included in Eqn (3.1). This equation have to be solved for each $\mathbf{k}$ point in the irreducible wedge of the Brillouin zone.

3.2 The linear augmented plane wave (LAPW)

The LAPW method [2]is not a fundamental modification of the APW of Slater [18]. Consequently, we shall first establish the essence and motivation of the Slater

[2]A detailed account of the LAPW method can be found in Ref. [17]

method as follows: The potential and wave functions in the vicinity of a nuclei vary strongly and are nearly spherical. On the contrary, they are smoother between the atoms. These observations lead to the division of the space into two regions where different kind of basis are used to represent the densities and potentials. Inside the non-overlapping atom centered spheres (S), radial solutions of the Schrödinger equation are used to describe the wave functions, whereas planewaves constitute a suitable basis in the remaining interstitial region,

$$\psi(\mathbf{r}) = \begin{cases} \frac{1}{\sqrt{\Omega}} \sum_{\mathbf{K}} a_{\mathbf{K}}\, e^{i(\mathbf{K}+\mathbf{k})\cdot\mathbf{r}} & \mathbf{r}\,\epsilon \text{ Interstitial}, \\ \sum_{lm} b_{lm}\, u_l(\mathbf{r})\, Y_{lm}(\mathbf{r}) & \mathbf{r}\,\epsilon \text{ S}. \end{cases} \tag{3.5}$$

In Eqn (3.5), Ω is the cell volume, $a_{\mathbf{K}}$ and b_{lm} are expansion coefficients, Y_{lm} are spherical harmonics and u_l is the regular solution of

$$\left(-\frac{\mathrm{d}^2}{\mathrm{d}r^2} + \frac{l(l+1)}{r^2} + V(r) - E_l\right) r\, u_l(r) = 0. \tag{3.6}$$

In Eqn (3.6) E_l is assumed to be a variable, not an eigenvalue and $V(r)$ is the spherical component of the potential in the sphere.

In order for the kinetic energy to be well defined the double representation of the basis in Eqn (3.5) must be continuous at the sphere boundary. This is accomplished in the APW by defining the coefficient b_{lm} in terms of $a_{\mathbf{K}}$ helped by the spherical harmonic expansion of the plane waves and subsequently, matching each coefficient b_{lm} at the sphere boundary. Thus the coefficients b_{lm} become

$$b_{lm} = \frac{4\pi i^l}{\sqrt{\Omega} u_l(R)} \sum_{\mathbf{K}} a_{\mathbf{K}}\, j_l(|\mathbf{K}+\mathbf{k}|R)\, Y_{lm}(\mathbf{K}+\mathbf{k}), \tag{3.7}$$

where the quantities $j_l(kr)$ are spherical Bessel functions of order l and R is the sphere radius. The coefficients b_{lm} are completely determined by the planewave coefficients and the energy variables E_l.

The planewaves in the interstitial region matched to the radial functions in the spheres constitute what we call the augmented planewaves or APWs. They are the solution of the Schrödinger equation inside the spheres for a given E_l. They do not posses the freedom to allow the wave function to adapt itself as the band energy deviates from the reference E_l. Therefore, the E_l must be set equal to the band energy ε, which makes the APWs energy dependent functions. Thus, the searching for the roots of the non-linear energy dependent [3] secular determinant

$$\det\left[H(E_l) - E_l\, \mathcal{O}(E_l)\right] = 0. \tag{3.8}$$

[3]The APW basis are energy dependent, so are the H and the $\mathcal{O}$ matrices represented in such basis.

must be achieved. This is a much more computationally demanding procedure than the single diagonalization of the secular matrix in Eqn (3.4) as it would be if the E_l were fixed parameters.

In the LAPW method [19], the exact solutions u_l for the spherical potential inside the spheres are replaced by linear combinations of $u_l(r)$ and its energy derivative $\dot{u}_l$. The wave functions written in terms of this basis are

$$\psi(\mathbf{r}) = \begin{cases} \dfrac{1}{\sqrt{\Omega}} \sum\limits_{\mathbf{K}} a_{\mathbf{K}}\, e^{i(\mathbf{K}+\mathbf{k})\cdot\mathbf{r}} & \mathbf{r}\,\epsilon \text{ Interstitial}, \\ \sum\limits_{lm} \left[b_{lm}\, u_l(\mathbf{r}) + d_{lm}\, \dot{u}_l(\mathbf{r})\right]\, Y_{lm}(\mathbf{r}) & \mathbf{r}\,\epsilon \text{ S}. \end{cases} \tag{3.9}$$

Here, the u_l are defined exactly as in APW, i.e. they are the solutions of the radial Schrödinger equation (see Eqn 3.6), with a fixed E_l and its energy derivative $\dot{u}_l$ satisfies

$$\left(-\frac{\mathrm{d}^2}{\mathrm{d}r^2} + \frac{l(l+1)}{r^2} + V(r) - E_l\right) r\,\dot{u}_l(r) = r\,u_l(r). \tag{3.10}$$

As in the APW, the wave functions must be continuous at the boundary and therefore the functions u_l and $\dot{u}$ are matched to the respective values and derivatives of the planewaves at the boundary.

The inclusion of $\dot{u}_l$ in the expansion of the wave function inside the sphere supplies more flexibility to the basis, which enables to represent all eigenstates in a region around E_l. For instance, if E_l differs slightly from the energy band ε, the radial function u_l at the energy band will be reproduced by a linear combination,

$$u_l(\varepsilon, r) = u_l(E_l, r) + (\varepsilon - E_l)\dot{u}_l(r) + \mathcal{O}((\varepsilon - E_l)^2). \tag{3.11}$$

In this way, all valance bands may be treated with a single set of E_l, leading to an energy independent basis set. Therefore, the secular equation becomes linear in energy and only a single diagonalization is needed to obtain accurate energy bands. The last fact constitutes a great advantage of LAPW compared with APW. However the price that LAPW pays due to its flexible basis is the loss of the optimal physical form of u_l inside the sphere, which implies a larger number of basis functions required to achieve convergence.

3.3 APW+local orbitals

An alternative linearization of APW was developed by Sjöstedt et al.[20], the so-called APW+lo method. One of the problems of the APW basis set is that it can only describe eigenstates with eigenenergies in the immediate vicinity of E_l. The situation improves in LAPW when modifying the augmented planewave inside the sphere, which adds more flexibility to the basis set. However the good representation of the wave function inside the spheres that APW possesses is lost.

APW+lo keeps the original APW basis set (Eqn (3.5)) with the exact radial solutions u_l of the Schrödinger equation inside the spheres evaluated at E_l but adds a complementary basis set, a set of local orbitals[17, 21],

$$\chi_{lo}(\mathbf{r}) = \begin{cases} 0 & \mathbf{r}\,\epsilon \text{ Interstitial,} \\ (b_{lm}\,u_l(\mathbf{r}) + d_{lm}\,\dot{u}_l(\mathbf{r}))\;Y_{lm}(\mathbf{r}) & \mathbf{r}\,\epsilon \text{ S.} \end{cases} \tag{3.12}$$

This extra basis set introduces the variational freedom. Local orbitals were brought into LAPW method to deal with semi-core states. Their local character comes from the fact that they are entirely confined to the spheres. Moreover, they have a specific lm character and are independent of $\mathbf{k}$ and $\mathbf{K}$. As in the former methods, the basis functions must be continuous and consequently local orbitals are matched at the boundary to zero, so it is obtained,

$$\frac{d_{lm}}{b_{lm}} = -\frac{u_l(R)}{\dot{u}_l(R)}, \tag{3.13}$$

where R is the sphere radius.

The APW+lo method uses both bases in such a manner that u_l is included as in APW to describe eigenstates whose eigenenergies are close to E_l and a linear combination of u_l and $\dot{u}_l$ for eigenstates of eigenenergies far away from E_l. Therefore the number of basis functions is considerable smaller than in the LAPW method yielding a faster convergence. Of course, for perfectly converged calculations both methods produce the same result.

Chapter 4

Non-collinear magnetism

4.1 Introduction

Solids contain magnetic moments that can act together cooperatively leading to a behaviour which is quite different from what would be observed if all the magnetic moments were isolated from each other. This collective behaviour and the diversity of types of magnetic interactions produce a surprisingly rich variety of magnetic properties in real systems. It is not the aim of this chapter to review the whole subject for that would be a tremendous task. Magnetic orderings in real materials will instead be our concern.

Different types of magnetic ground state order can be found as a direct consequence of the different types of exchange interactions that operate between the magnetic moments in a solid. Some of them are illustrated in Fig. 4.1. The first two spin arrangements are commonly called collinear structures, for there is a global spin quantization axis along which all the spins in the structure align either parallel or anti-parallel. The last three of these structures in Fig. 4.1 are characterized by the lack of such a global axis and they are classified as non-collinear structures. We will focus on the latter type of magnetic order in this chapter, especially spin spirals.

4.2 Spin Spirals

A spin spiral structure as depicted in Fig. 4.1d can be defined by expressing the Cartesian coordinates of the magnetization density as

$$\mathbf{m}(\mathbf{r}) = m(\mathbf{r}) \left[\cos(\mathbf{q}\cdot\mathbf{R}+\varphi)\sin\theta,\, \sin(\mathbf{q}\cdot\mathbf{R}+\varphi)\sin\theta,\, \cos\theta\right], \qquad (4.1)$$

where m is the magnitude of the magnetic moment, φ and θ are polar angles, $\mathbf{R}$ is a lattice vector and $\mathbf{q}$ is the wave vector that characterizes the spin spiral. A distinctive property of the spiral structure is the lack of translational symmetry along the direction of the wave vector $\mathbf{q}$. Nevertheless, a close look at Eqn (4.1) reveals that all atoms of the spiral structure separated by a translation $\mathbf{R}$ posses magnetic

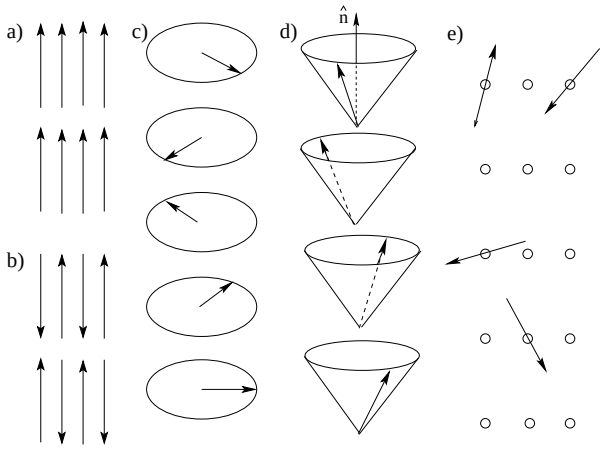

Figure 4.1: Various spin arrangements in ordered systems: (a) ferromagnet, (b) antiferromagnet, (c) helical structure, (d) spin spiral and (e) spin glasses.

moments of the same magnitude and hence they are equivalent. This equivalence gives rise to an interesting property for the single-particle spinors functions (Eqn 2.13).

Indeed, as was first pointed out by Herring [22] and later by Sandratskii [23, 24], transformations combining a lattice translation $\mathrm{T}_{\mathbf{R}}$ and a spin rotation about the spiral axis $\hat{n}$ (see Fig. 4.1) by an angle $\phi = \mathbf{q} \cdot \mathbf{R}$ leave the spiral structure invariant,

$$\mathcal{T}_{\phi}\, \mathbf{m}(\mathbf{r}) = \mathbf{m}(\mathbf{r}). \tag{4.2}$$

The symmetry operators that describe these transformations belong to a spin-space group (SSG)[1]. Three important properties of these generalized translations, can be stated as follows i) spinors transform according to

$$\mathcal{T}_{\phi}\, \psi(\mathbf{r}) = \begin{pmatrix} e^{-i\mathbf{q}\cdot\mathbf{R}/2} & 0 \\ 0 & e^{i\mathbf{q}\cdot\mathbf{R}/2} \end{pmatrix} \psi(\mathbf{r} - \mathbf{R}), \tag{4.3}$$

ii) they commute with the Kohn-Sham Hamiltonian (see Eqn 2.30) of a spin spiral structure, and iii) they form an Abelian group isomorphic to the group of ordinary space translations $\mathrm{T}_{\mathbf{R}}$. Therefore, they have the same irreducible representation, which as we know, constitutes the Bloch Theorem in the case of ordinary space translations. The generalized Bloch theorem is then established as

$$\mathcal{T}_{\phi}\psi_{\mathbf{k}}(\mathbf{r}) = e^{-i\mathbf{k}\cdot\mathbf{R}}\, \psi_{\mathbf{k}}(\mathbf{r}). \tag{4.4}$$

These properties enable us to express the generalized Bloch spinors [22] that diag-

[1] A detailed description of this theory can be found in [25].

onalize the spiral Hamiltonian $\mathcal{H}$ as [2]

$$\psi_{\mathbf{k}}(\mathbf{r}) = e^{i\mathbf{k}\cdot\mathbf{r}} \begin{pmatrix} e^{-i\mathbf{q}\cdot\mathbf{r}/2}\alpha_{\mathbf{k}}(\mathbf{r}) \\ e^{i\mathbf{q}\cdot\mathbf{r}/2} \ \beta_{\mathbf{k}}(\mathbf{r}) \end{pmatrix} \tag{4.5}$$

where $\alpha_{\mathbf{k}}$ and $\beta_{\mathbf{k}}$ are the periodic functions for the spin-up and spin-down components respectively. These generalized spinors will produce the same charge density as the ordinary spinors and the magnetization density as defined in Eqn (4.1). The generalized symmetry group permits us to solve the Kohn-Sham equations (Eqn (2.18)) in the presence of spin spirals without using supercells. In this way, we have recovered the symmetry of the chemical unit cell.

Unfortunately, the fast Fourier transforms that full-potential methods use require translational invariant potentials and densities. Nordström [26] developed a slightly different scheme, which incorporates naturally the spin spiral symmetries. Two new complex quantities are introduced, u and h, with the spin axis taken in the z-direction [3]

$$u(\mathbf{r}) = e^{-i\mathbf{q}\cdot\mathbf{r}} \left(m_x(\mathbf{r}) + i\, m_y(\mathbf{r})\right) \tag{4.6}$$

$$h(\mathbf{r}) = e^{-i\mathbf{q}\cdot\mathbf{r}} \left(b_x(\mathbf{r}) + i\, b_y(\mathbf{r})\right) \tag{4.7}$$

where m_x and m_y are the perpendicular components of the magnetization density and b_x and b_y are the corresponding magnetic field components. The new quantity h is used now to write the Kohn-Sham Hamiltonian, which takes the form of (see Eqn (2.30)),

$$\mathcal{H} = (-\nabla^2 + v^{\text{nm}})\mathbb{1} + \frac{1}{2}\left(e^{i\mathbf{q}\cdot\mathbf{r}}\, h(\mathbf{r})\sigma_- + e^{-i\mathbf{q}\cdot\mathbf{r}}\, h^\dagger(\mathbf{r})\sigma_+\right) + b_z\sigma_z \tag{4.8}$$

with

$$\sigma_- = \sigma_x - i\sigma_y \qquad \text{and} \qquad \sigma_+ = \sigma_y + i\sigma_x. \tag{4.9}$$

Finally, we can easily obtain the density u from the generalized Bloch spinors as defined above,

$$u(\mathbf{r}) = \sum_{j,\mathbf{k}} \psi^\dagger_{j,\mathbf{k}} \left(e^{-i\mathbf{q}\cdot\mathbf{r}}\, \sigma_+\right)\, \psi_{j,\mathbf{k}}. \tag{4.10}$$

These quantities are invariant under the ordinary space translations by construction, and hence can be implemented in full-potential methods with normal Fourier transforms.

[2] We will show later how the form of the spinor wave functions has important implications in the origin of non-collinear magnetism.

[3] In the absence of the spin-orbital term, $\hat{n}$ can be taken arbitrarily along the z-direction without any loss of generality.

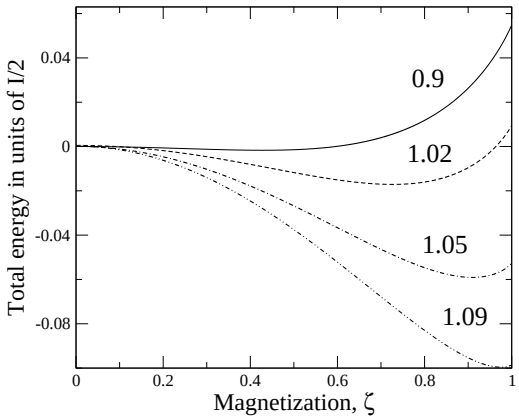

Figure 4.2: The total energy as a function of the magnetization for some values of $\mathcal{N}_0 I$, which are displayed on top of every curve in the figure.

4.3 Origin of the magnetic ordering

The nature of the magnetic ordering in solids is, despite decades of research, not understood on a microscopic level. In particular it is not known why one in Nature most often observes collinear magnets and only in few cases non-collinear magnetic ordering. Before this question is addressed we shall briefly analyze the conditions for magnetism to appear. The important role of the magnetic susceptibility as a signal of magnetic instabilities will be introduced. In the end, we shall discuss the concept of Fermi surface nesting as a crucial factor in the stabilization of the spin spiral structure.

4.3.1 Itinerant electron theory (Stoner criterion)

The magnetism of the majority of the metallic magnets, excluding those involving rare earths, can be understood in the itinerant electron picture. Stoner theory of itinerant magnetism [27, 28] describes electrons which move in the periodic potential of the solid and are characterized by the quantum number n, $\mathbf{k}$ and $\sigma_\pm$ i.e. the band index, the wave vector and a spin projection.

Our aim is to probe the stability of the non-magnetic state by introducing a molecular field which contains all exchange interactions. In analogy with the Weiss model [4] the molecular magnetic field is written as

$$H_m = I\zeta, \tag{4.11}$$

where I and ζ denote the molecular field constant and the magnetization respectively. The total energy of the electrons moving in the molecular field contains

[4] A complete description of Weiss model can be found in [29].

contributions from the kinetic and the field energy. By assuming that the electrons move in a s-band,[5] where the density of states is proportional to $\sqrt{\varepsilon}$, the total energy can be written as a function of ζ as

$$E(\zeta) = \frac{9}{20\mathcal{N}_0}\left[(1+\zeta)^{5/3} + (1-\zeta)^{5/3}\right] - \frac{I}{2}\zeta^2, \tag{4.12}$$

where $\mathcal{N}_0$ is the density of states at the Fermi energy. It is possible to see in Fig. 4.2, where the total energy for different values of $\mathcal{N}_0 I$ has been plotted, that as the value of $\mathcal{N}_0 I$ grows larger than one, a minimum in the total energy for a finite value of ζ develops, i.e. a spontaneous magnetization appears in the system. Therefore, in order for the non-magnetic state to become unstable, the second derivative of the total energy must be negative at $\zeta = 0$, which leads to

$$\mathcal{N}_0 I > 1. \tag{4.13}$$

This relation is called the Stoner condition and is fulfilled when the density of states at the Fermi energy is large[6]. Therefore the phase transition from the non-magnetic state to the ferromagnetic state is usually caused by a peak in the density of state at the Fermi energy.

The Stoner condition manifests itself as well in the enhanced susceptibility, which can be obtained from the total energy in the non-magnetic limit $\zeta \to 0$ as

$$\chi = \lim_{\zeta\to 0}\left(\frac{\mathrm{d}^2 E}{\mathrm{d}\zeta^2}\right)^{-1} = \frac{\mathcal{N}_0}{1 - I\mathcal{N}_0}. \tag{4.14}$$

The enhanced susceptibility in Eqn (4.14) can be rewritten as the product of the Pauli susceptibility, χ_p, times an enhancement factor which represents the fact that the susceptibility of a interacting electron system can not be determined merely by the Pauli susceptibility alone. The denominator of the enhanced susceptibility becomes very small for metals near a magnetic instability.

The derivation given above follows the original work of Stoner. The enhanced magnetic susceptibility as well as the Stoner condition can be re-obtained in a more contemporary way from DFT. In this context an expression is derived for the Stoner factor I, which is now seen as an exchange-correlation integral, and it is simply called the Stoner exchange constant[7].

4.3.2 The static nonuniform magnetic susceptibility

In this and the next sections we shall explore the conditions of magnetic instabilities that could produce eventually spin spiral structures. In the former section,

[5] This choice was made only for computational convenience. In reality the electron states leading to magnetism originate from d bands.

[6] It has been found that the molecular field constant is of the same order of magnitude for most of metals.

[7] A detailed derivation of the Stoner exchange constant can be found in Refs. [4, 29].

we found that the magnetic susceptibility plays an important role as an indicator of instabilities. The magnetic susceptibility is an example of a more general concept, namely, the linear response functions. Here we are interested, in particular, in the magnetic response of the inhomogeneous system to an external static magnetic field that is non-uniform in space. If the magnitude of the field is small, we can assume the response, χ to be linear. In general, we can write the induced magnetization as

$$\delta m(\mathbf{r}) = \int \chi(\mathbf{r}, \mathbf{r}')\, \delta B(\mathbf{r}')\, \mathrm{d}\mathbf{r}'. \tag{4.15}$$

Sandratskii and Kübler [30] addressed this problem within the LDFT approximation by specifying a magnetic field whose spatial variation is characterized by the vector $\mathbf{q}$,

$$\Delta\mathbf{B}(\mathbf{r}) = \Delta B \sum_n (\cos(\mathbf{q}\cdot\mathbf{R}),\, \sin(\mathbf{q}\cdot\mathbf{R}),\, 0)\; \Theta(|\mathbf{r}-\mathbf{R}|), \tag{4.16}$$

where $\Theta(r)$ is the unit step function which is 1 for r smaller than the atomic sphere radius and zero otherwise. The magnetic field specified above favours a spiral with $\theta = 90$ (see Eqn (4.1)). They obtained the enhanced susceptibility[8] for static magnetic fields parallel to the magnetization density at each point,

$$\chi = \frac{\chi_0(\mathbf{q})}{1 - I(\mathbf{q})\chi_0\mathbf{q}}, \tag{4.17}$$

with

$$I(\mathbf{q}) = \chi_0(\mathbf{q})^{-1} - \chi(\mathbf{q})^{-1} \tag{4.18}$$

where $\chi_0(\mathbf{q})$ is the susceptibility of non-interacting uniform electrons gas. Eqns (4.17) and (4.18) must be then solved self-consistently.

4.3.3 Fermi surface nesting

We shall now examine a Fermi surface feature of fundamental interest, the nesting. The Fermi surface nesting can largely influence the magnetic susceptibility and therefore it constitutes a decisive factor in the study of magnetic instabilities.

Let us start from Eqn (4.17). In order to obtain an expression for χ_0, the so-called Lindhard expression in its non-magnetic state is used, which in this case describes the response function for noninteracting electrons as,

$$\chi^0(\mathbf{r}, \mathbf{r}') = \sum_{\mathbf{k}\mu}\sum_{\mathbf{k}'\nu} \frac{\Theta(\varepsilon_\mathrm{F} - \varepsilon_{\mathbf{k}\mu}) - \Theta(\varepsilon_\mathrm{F} - \varepsilon_{\mathbf{k}'\nu})}{\varepsilon_{\mathbf{k}\mu} - \varepsilon_{\mathbf{k}'\nu}} \times \\ \times \psi_{\mathbf{k}\mu}(\mathbf{r})\psi^*_{\mathbf{k}\mu}(\mathbf{r}')\psi_{\mathbf{k}'\nu}(\mathbf{r}')\psi^*_{\mathbf{k}'\nu}(\mathbf{r}). \tag{4.19}$$

[8] A complete derivation is given in Ref. [4].

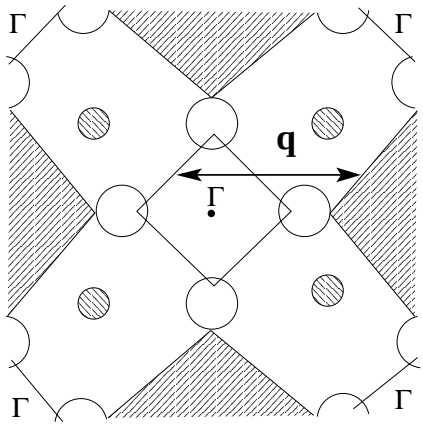

Figure 4.3: Schematic Fermi surface cross-section. The arrow shows the $\mathbf{q}$-vector that separates two parallel portions of electron and hole Fermi surfaces.

Here $\Theta(x)$ is the unit step function and ν and μ are band indices and k and k' are wave vectors that label Bloch states. By applying the Fourier transform twice to this equation we obtain (see ref.[3]),

$$\begin{aligned} \chi^0(\mathbf{q},\mathbf{q}') &= \iint e^{-i\mathbf{q}\cdot\mathbf{r}} e^{-i\mathbf{q}'\cdot\mathbf{r}'} \chi^0(\mathbf{r},\mathbf{r}')\,\mathrm{d}\mathbf{r}\,\mathrm{d}\mathbf{r}' \\ &= \delta_{\mathbf{q},\mathbf{q}'}\chi_0(\mathbf{q}) \end{aligned} \tag{4.20}$$

where

$$\chi_0(\mathbf{q}) = \sum_{\mathbf{k}\mu\nu} \frac{[f(\varepsilon_{\mathbf{k}\nu}) - f(\varepsilon_{\mathbf{k}-\mathbf{q}\mu})]}{\varepsilon_{\mathbf{k}-\mathbf{q}\mu} - \varepsilon_{\mathbf{k}'\nu} + i\delta} \cdot |\langle \mathbf{k}\nu | e^{i\mathbf{q}\cdot\mathbf{r}} | \mathbf{k}-\mathbf{q}\mu\rangle|^2. \tag{4.21}$$

The expression in Eqn (4.21) was generalized by using the Fermi distribution $f(\varepsilon)$ instead of the $\Theta(x)$ function and an infinitesimal $i\delta$. The denominator in Eqn (4.21) becomes very small if there exist parallel portions of electron and hole Fermi surfaces that, by a rigid shift defined by a vector $\mathbf{q}$, can be brought together to coincide (see Fig. 4.3). This feature of the Fermi surfaces is called nesting. It should be noted that in the case of strong nesting and low temperature, $\chi_0(\mathbf{q})$ becomes very large since the denominator in Eqn (4.21) is almost zero for many values of $\mathbf{k}$ in the sum and the numerator is close to one. Therefore, the magnetic susceptibility $\chi(\mathbf{q})$ can become very large for the value of $\mathbf{q}$ that defines the Fermi nesting shift. Thus we can obtain a generalized Stoner condition

$$I\chi_0(\mathbf{q}) \geq 1, \tag{4.22}$$

which again indicates an instability of the non-magnetic state. Fig. 4.3 represents a schematic Fermi surface cross-section, where the $\mathbf{q}$-vector that separates the portions of electron and hole Fermi surfaces, has been identified. It is worth noticing

that the magnitude of $\mathbf{q}$ in Fig. 4.3 is less than the reciprocal lattice vector magnitude $\overrightarrow{\Gamma H}$, which means that the adopted spin spiral structure will not be commensurate with the lattice. The Fermi surface nesting has been proved to have a large effect in the susceptibility, which in turns, provides us with a signal of a magnetic instability.

In paper II we will describe a new mechanism of stabilization of spin spiral structures in metals, which involves the shape of the spinor wave functions and nesting Fermi surface features.

Chapter 5

Results

Two works presented in this thesis are included at the end. This chapter is dedicated to review some of the most relevant aspects of them and with that purpose, it has been divided in two parts. The first part is devoted to paper I, where the magnetic structure of the $TlCo_2Se_2$ compound is investigated from an experimental and a theoretical point of view. The analysis given here though, will only contain a theoretical discussion.

Why do atomic spins arrange ferromagnetically or antiferromagnetically whereas only in few occasions, do they choose to order in a non-collinear way? This is a question that despite decades of research has not found a complete answer yet. The second part of this chapter, paper II, deals with this question.

In both papers, first principles calculations were performed using the APW+lo method, that was discussed extensively in chapter 3. In paper II a non-collinear LMTO-ASA method [31] was employed as well to carry out some of the calculations.

5.1 Paper I

Complex magnetic behaviour can be found in low dimensional systems. Nowadays, high technology has been developed that permits us to built artificially low dimensional magnets, for example, ferromagnetic multilayer or thin films. Nevertheless, low dimensionality can also occur naturally in some systems. Some crystals grow in such a manner that the magnetic atoms or ions are located in layers. Such is the case of $TlCo_2Se_2$, which adopts the layered tetragonal $ThCr_2Si_2$ (space group I4/mmm) crystal structure[1]. Composition and atomic distances influence largely the type of magnetic order observed in the $ThCr_2Si_2$-type family. The magnetism in $TlCo_2Se_2$ is driven by the cobalt atoms which sit in square lattices in two dimensions in the crystal structure. Its magnetic structure is displayed in Fig. 5.1, however thallium and selenium atoms have been omitted since they do not contribute significantly to the total magnetic moment. According to the study

[1]The crystal structure of $TlCo_2Se_2$ is depicted in paper I.

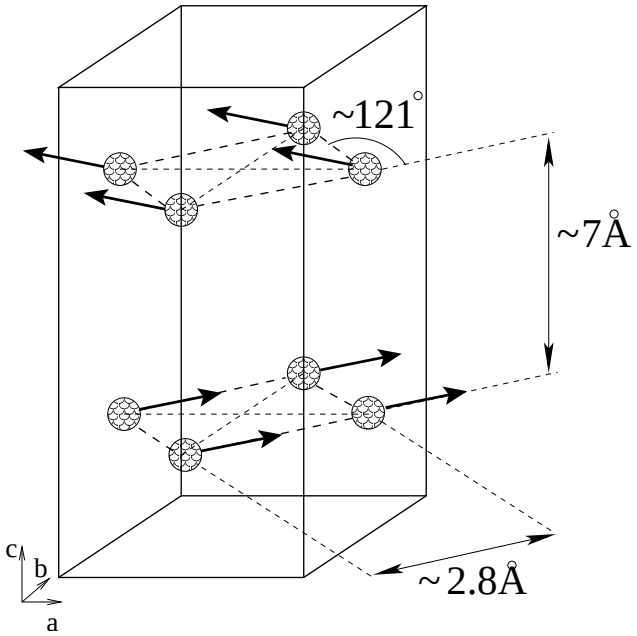

Figure 5.1: The magnetic structure of the $TlCo_2Se_2$ compound, where only the cobalt atoms are displayed in the figure. The magnetic moments of the cobalt atoms are arranged ferromagnetically within each layer and perpendicular to the c-axis. An incommensurate helix runs along the c-axis with a turn angle of $\sim 121^\circ$, as it is indicated by the arrows on the cobalt atoms.

performed by Berger et al. [32], the cobalt atoms arrange ferromagnetically within the layers and a helical structure develops along the c-axis with a turn angle [2] of $\sim 121^\circ$. The cobalt magnetic moments lie in the ab plane. Since the experimental model proposed by Berger et al. was deduced from weak magnetic contributions from the powder diffraction pattern, a single-crystal investigation was suggested. The aim of paper I is then to explore further the magnetism in the $TlCo_2Se_2$ by means of single-crystal diffraction experiments and first principles calculations.

The calculated total energy is shown in Fig.5.2 as a function of the value of q,

$$\mathbf{q} = (0, 0, q)\frac{2\pi}{c}, \tag{5.1}$$

relative to the energy of the ferromagnetic state. Different values of q represent different magnetic structures. A ferromagnetic state is obtained when $q = 0$ whereas $q = 1$ corresponds to an antiferromagnetic state. Each q-value in between these two values of q characterize different spin spirals. The minimum in the energy curve (Fig.5.2) at $q = 1$ indicates that the ground state corresponds to the antifer-

[2] The turn angle is defined as the angle between the magnetic moments of each layer, $\phi = \mathbf{q} \cdot \mathbf{R}$, where $\mathbf{R}$ stands for a translation lattice vector and $\mathbf{q}$ is the spin spiral wave vector that characterizes the spiral structure. More details are given in chapter four.

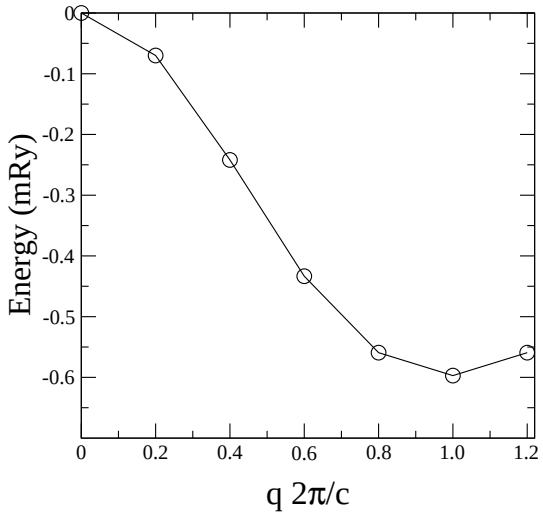

Figure 5.2: Total energy as a function of the value of q, relative to the energy of the ferromagnetic structure ($q = 0$).

romagnetic configuration. This result does not quite agree with the powder neutron diffraction result of a helical structure, which is supported by the single-crystal diffraction data[3]. However, it can be observed in Fig.5.2 that there is a small difference, ≈ 0.1 mRy, between the energy of the experimental non-collinear structure and the antiferromagnetic configuration. The cobalt magnetic moment was determined to be $\approx 0.5\mu_{\mathrm{B}}$ which is in almost perfect agreement with neutron diffraction data. Thallium and selenium atoms have no significant contribution to the total magnetic moment.

5.2 Paper II

The most common theoretical explanations for non-collinear magnetic ordering involve either magnetic frustration in materials with crystal structures that have anti-ferromagnetic exchange interactions [4] or nearest neighbour ferromagnetic interactions that are of similar size to next nearest neighbour anti-ferromagnetic interactions [33]. For the late rare-earths the RKKY interaction has also been argued to cause non-collinear states [34]. In paper II, two criteria are identified which determine whether a magnetic metal may be stabilized in a collinear or non-collinear arrangement.

To illustrate these ideas, a schematic energy band of a hypothetical element is displayed in Fig. 5.3. In a ferromagnetic state, spin up and spin down bands are orthogonal and therefore they can not hybridize. This is represented by black and light gray straight lines in Fig. 5.3. However, as it was discussed in chapter two,

[3]The results obtained by this experiments are detailed in paper I.

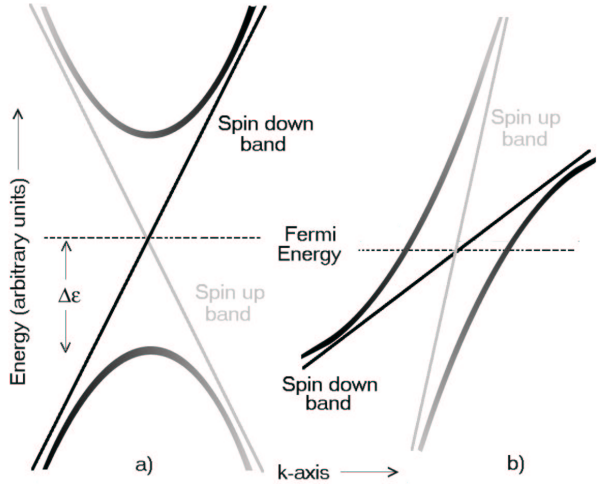

Figure 5.3: Schematic energy band structures of a hypothetical element. The black and light gray straight lines stand for two orthogonal spin down and up bands respectively in the ferromagnetic state. The presence of a non-collinear coupling permits the hybridization of the two spin channels and the hybridized bands become the gray-gradient, curved lines. The dashed horizontal line represents the Fermi energy. Two different possibilities are shown in figure a) and b).

in the more general non-collinear formulation the one-electron states do not possess pure spin up or down character and the wave functions are described by two component spinors (see Eqn (2.13)). In the case of spirals, the generalized Bloch spinors that diagonalize the spiral Hamiltonian were given in Eqn (4.5). Consequently, the presence of a non-collinear magnetic coupling such as in a spin spiral state, allows the two spin components to hybridize. Such hybridization is depicted in Fig. 5.3 as the gray-gradient parabolic curves. These two bands experience repulsion which opens up an energy gap. If the hybridization gap occurs at the Fermi energy, the band that has been pushed down will lower the total energy whereas the band that has been pushed up will not contribute to the total energy, since it is now empty. Fig 5.3b presents a similar situation but the mechanism that lowers the total energy is not as efficient as in Fig 5.3a.

Two criteria for the formation of spin spirals can be deduced from the mechanism sketched above. First, the Fermi energy should cut through both spin up and down states. This condition excludes immediately strong ferromagnets such as bcc Fe, hcp Co and fcc Ni, where the spin up band is filled. In contrast, spin spirals are expected to be observed in fcc Fe, bcc Mn and fcc Mn at ambient conditions. Secondly, the mechanism discussed in Fig. 5.3 is extra efficient if there is nesting features[4] between spin up and spin down states. In that case, large areas of the spin up and down Fermi surfaces can be brought together by a rigid shift in k-space of

[4]Fermi surfaces nesting was disscused in some detail in chapter four.

length q. This guarantees that many k-points are involved in the energy lowering process discussed above.

A simple model calculation can be carried out to estimate the hybridization gap. The non-collinear component of the Hamiltonian, denoted by U, that gives rise to the hybridization corresponds, in a matrix representation, to the off-diagonal elements and will be considered for simplicity as a small perturbation to a ferromagnetic configuration of a material with free electron like band states. Thus, by using the wave function defined in Eqn (4.5) the resulting eigenvalue problem [35] of this simple model can be written as

$$\begin{pmatrix} \lambda_{\mathbf{k}-\mathbf{q}/2} - \varepsilon & U \\ U & \lambda_{\mathbf{k}+\mathbf{q}/2} - \varepsilon \end{pmatrix} \begin{pmatrix} e^{i(\mathbf{k}-\mathbf{q}/2)\cdot\mathbf{r}}\alpha_{\mathbf{k}} \\ e^{i(\mathbf{k}+\mathbf{q}/2)\cdot\mathbf{r}}\beta_{\mathbf{k}} \end{pmatrix} = 0, \tag{5.2}$$

where $\lambda_{\mathbf{k}} = \hbar^2 k^2/2m$ corresponds to the eigenvalue of the free electron bands. As usual, a non-zero solution of Eqn (5.2) requires the determination of the roots of the secular determinant. Such a procedure, after some algebra, yields an expression for the two roots $\varepsilon_{\pm}$,

$$\varepsilon_{\pm} \approx \frac{\hbar^2}{2m}\left(k^2 + \frac{q^2}{4}\right) \pm U\left(1 + \frac{1}{2}\left(\frac{\hbar}{2m}\right)^2 \frac{(\mathbf{k}\cdot\mathbf{q})^2}{U^2}\right). \tag{5.3}$$

It was assumed in Eq. (5.3) that $|U| \ll \hbar(\mathbf{k}\cdot\mathbf{q})/2m$. Each root in Eq. (5.3) describes an energy band as shown in Fig. 5.3. The solution ε_- corresponds to the lower energy of the two bands. Consequently, the hybridization gap $\Delta\varepsilon$ (see Fig. 5.3), can be determined by evaluating the difference between the Fermi energy, and ε_- at the Fermi wavevector k_{F}, defined as the k-point where the spin up and and spin down bands cross the Fermi energy (see Fig. 5.3),

$$\Delta\varepsilon = \frac{\hbar^2}{2m}\mathbf{k}_{\mathrm{F}}^2 - \varepsilon_- = -\frac{\hbar}{2m}\frac{q^2}{4} + U + \frac{1}{2}\left(\frac{\hbar}{2m}\right)^2 \frac{(\mathbf{k}\cdot\mathbf{q})^2}{U}. \tag{5.4}$$

It is clear that a larger gap causes a larger effect in lowering the total energy, and we have identified a mechanism that stabilizes the non-collinear configuration.

Therefore, non-collinear systems are expected to occur provided that one can tune the exchange splitting and/or the band filling. First principles calculations were performed for several transition metal where the tuning of the exchange splitting was made either by modifying the volume or by using the so called fixed spin moment method[36]. All elements that have been investigated, bcc V, bcc and fcc Mn, bcc and fcc Fe, bcc and fcc Co, as well as bcc and fcc Ni, are found to favour a non-collinear state after tuning the exchange splitting so that the mechanism illustrated in Fig. 5.3 becomes operative.

Our analysis shows that a non-collinear state can be stabilized in any element or compound provided the band filling and exchange splitting are tuned correctly. This conclusion holds irrespective of the chemical composition of the material or

the nature of the crystal structure. This means that complex magnetic structures may indeed be found even though the crystal geometry in it-self does not give rise to magnetic frustration.

Acknowledgments

Embarking in a new project is always a challenge, specially if large and deep changes in one's life are involved. Starting postgraduate studies in Sweden has been a big challenge for me. The conclusion of this first part of my time here, is not solely an achievement of myself. Many people have contributed in one way or another to make this moment possible and this is the time and place to say thanks.

First, I would like to thank my parents for loving me and supporting my projects and ideas even though that means to have me far away from them.

It is difficult to put in words what Erik's love, patience and putting up with my complaining have meant to me. Thanks Bandi, none of this would have been accomplished without you!

Thanks very much to my brothers, Jorge and Cristian, for cheering me up with their jokes and funny e-mails... however it is not necessary to send two copies of each joke!!

I am tremendously grateful to my supervisors Olle Eriksson and Lars Nordström for their support, help, confidence and never-ending encouraging. I have learnt a lot from you. Although being a very busy person, Olle always finds two seconds to talk with his students, or ask you a question that will open an interesting discussion. I must confess that some of those question's significations have remained hidden for me. For instance, I am still puzzled trying to figure out what is the deepest meaning of ¿Dónde estan los caballeros?!!...

I really appreciate the effort that Börje Johansson and Olle Eriksson put in making of our group, fysik4, a very pleasant place to work in. Of course, their work would be just incomplete if it would not be for the members of the group. I am very thankful to all of them, Ph. D students, seniors, system administrators and people that already left the group. I would like to thank Lars N and Bettan, who spent some time (maybe more than some) with me in the turns and twists of the APW+lo code. A special thanks goes to Weine, Björn, Lars B, Carlos, Thomas and Alexei. It must not be easy to keep running a big cluster of computers with more than thirty users!

I also would like to express my gratitude, to my friends in Uppsala, Paula, Cecilia, Arantxa, Mauro, Jorge and Gloria. Thanks for your affection and companion.

A big 'Shilemublare' to Erik's family for making me feel at home. Probably

this is not the spelling you would have picked for this interesting concept. I just want to say that I did my best.

Thanks Ana, for dinner, thesis-advise and for always having time for a coke and a nice chatting.

Bibliography

[1] S. Blundell, *Magnetism in Condensed Matter* (Oxford University Press, Oxford, 2001).

[2] N. Ashcroft and D. Mermin, *Solid State Physics* (Saunders College Publishing, New York, 1976).

[3] W. Jones and N. March, *Theoretical solid state physics* (John Wiley & Sons, London, 1973).

[4] J. Kübler, *Theory of Itinerant Magnetism* (Oxford Science Publications, Clarendon Press, Oxford, 2000).

[5] P. Hohenberg and W. Kohn, Phys. Rev. B **136**, 864 (1964).

[6] W. Kohn and L. Sham, Phys. Rev. A **140**, 1133 (1965).

[7] U. von Barth, *Electronic Structure of Complex Systems* (Plenum, New York, 1984).

[8] J. Callway and N. March, *Solid State Physics* (Academic Press, Orland, 1984).

[9] R. Dreizler and E. Gross, *Density functional theory* (Springer-Verlag, Berlin, 1990).

[10] D. C. Langreth and M. J. Mehl, Phys. Rev. B **28**, 1809 (1993).

[11] A. D. Becke, Phys. Rev. A **38**, 3898 (1988).

[12] J. P. Perdew *et al.*, Phys. Rev. B **46**, 6671 (1992).

[13] O. Gunnarsson, M. Jonson, and B. Lundqvist, Solid State Comunication **24**, 765 (1977).

[14] O. Gunnarsson, M. Jonson, and B. Lundqvist, Phys. Rev. B **20**, 3136 (1979).

[15] O. Gunnarsson and R. O. Jones, Phys. Scr. **21**, 394 (1980).

[16] U. von Barth and L. Hedin, J. Phys. C:Sol. State Phys. **5**, 1629 (1972).

[17] D. Singh, *Planewaves, pseudopotentials and the LAPW method* (Kluwer Academic Publishers, Massachusetts, 1984).

[18] J. C. Slater, Phys. Rev. **51**, 846 (1937).

[19] O. K. Andersen, Phys. Rev. B **12**, 3060 (1975).

[20] E. Sjöstedt, L. Nordström, and D. Singh, Sol. State. Com. **114**, 15 (2000).

[21] D. J. Singh, Phys. Rev. B **43**, 3060 (1991).

[22] C. Herring, *Magnetism, exchange interactions among itinerant electrons* (Academic Press, New York and London, 1966).

[23] L. Sandratskii, Phys. Stat. Sol. (b) **135**, 167 (1986).

[24] L. Sandratskii, J. Phys. F: Metal Phys. **16**, L43 (1986).

[25] L. Sandratskii, Advances in Physics **47**, 91 (1998).

[26] L. Nordström and A. Mavromaras, Europhys. Lett. **49**, 775 (2000).

[27] E. C. Stoner, Proc. Roy. Soc. London A **165**, 372 (1938).

[28] E. C. Stoner, Proc. Roy. Soc. London A **169**, 339 (1939).

[29] P. Mohn, *Magnetism in the Solid State, an introduction* (Springer-Verlag, Berlin, 2003).

[30] L. Sandratskii and J. Kübler, J. Phys. Condens. Matter **4**, 6927 (1992).

[31] L. Bergqvist (for details see www.fysik.uu.se\theomag).

[32] R. Berger *et al.*, J. Alloys Comp. **343**, 186 (2002).

[33] J. Jensen and A. Mackintosh, *Rare earth magnetism* (Oxford University press, Oxford, 1991).

[34] R. Elliot and F. Wedgwood, Proc. Phys. Soc. **81**, 846 (1963).

[35] C. Kittel, *Introduction to Solid State Physics* (John & Sons, Inc. Seventh edition, New York, 1996).

[36] K. Schwarz and P. Mohn, J. Phys. F **14**, L129 (1984).